



University of Kurdistan

Dept. of Electrical and Computer Engineering

Smart/Micro Grid Research Center

smgrc.uok.ac.ir

On Load–Frequency Regulation With Time Delays: Design and Real-Time Implementation

H. Bevrani, G. Ledwich, Z. Y. Dong, J. J. Ford

Published (to be published) in: ***IEEE Transactions on Energy Conversion***

(Expected) publication date: **2009**

Citation format for published version:

Bevrani, Hassan & Hiyama, Takashi (2009) On Load-Frequency Regulation with Time Delays: Design and Real Time Implementation. *IEEE Transactions on Energy Conversion*, vol. 24(1), pp. 292-300, Jan 2009, DOI: 10.1109/TEC.2008.2003205

Copyright policies:

- Download and print one copy of this material for the purpose of private study or research is permitted.
- Permission to further distributing the material for advertising or promotional purposes or use it for any profit-making activity or commercial gain, must be obtained from the main publisher.
- If you believe that this document breaches copyright please contact us at smgrc@uok.ac.ir providing details, and we will remove access to the work immediately and investigate your claim.

On Load–Frequency Regulation With Time Delays: Design and Real-Time Implementation

Hassan Bevrani, *Senior Member, IEEE*, and Takashi Hiyama, *Senior Member, IEEE*

Abstract—This paper addresses a robust decentralized proportional-integral (PI) control design for power system load–frequency regulation with communication delays. In the proposed methodology, the PI-based load–frequency control (LFC) problem is reduced to a static output feedback control synthesis for a multiple-delay system. The proposed control method gives a suboptimal solution using a developed iterative linear matrix inequalities algorithm via the mixed H_2/H_∞ control technique. The control strategy is suitable for LFC applications that usually employ the PI control. To demonstrate the efficiency of the proposed control strategy, an experimental study has been performed at the Research Laboratory, Kyushu Electric Power Company, Japan.

Index Terms—Frequency regulation, linear matrix inequality (LMI), mixed H_2/H_∞ , robust performance, static output feedback (SOF) control, time delay.

I. INTRODUCTION

REAL-WORLD load–frequency regulation systems usually use the proportional-integral (PI) type controllers. Since the PI controller parameters are commonly tuned based on classical, experiences, and trial-and-error approaches, they are incapable of obtaining good dynamical performance for a wide range of operating conditions and various load scenarios.

ON the other hand, the power system frequency regulation systems, known as load–frequency control (LFC) systems, are faced by new uncertainties in the liberalized electricity market. The modeling of these uncertainties and dynamic behavior to design suitable controllers is very important. An effective power system market needs an open communication infrastructure to support the increasing decentralized property of control processes. Therefore, in the near future, the communication delay will become one of significant uncertainties in the LFC synthesis/analysis due to expanding physical setups, functionality, and complexity of a power system; as a result, the time delays can degrade a system’s performance and even cause system instability [1]–[3].

Recently, several papers have been published to address the LFC modeling/synthesis in the presence of communication delays [4]–[6]. In [4], the focus is on the network delay models

and communication network requirement for a third party LFC service. A compensation method for communication time delay in the LFC systems is addressed in [5] and a control design method based on linear matrix inequalities (LMIs) is proposed for the LFC system with communication delays in [6]. Most published research works on the PI-based LFC have neglected problems associated with the communication network. Although, under the traditional dedicated communication links, this was a valid assumption, the use of an open communication infrastructure to support the ancillary services in deregulated environments raises concerns about problems that may arise in the communication system.

The authors in [7] have proposed a robust decentralized H_∞ control strategy for the designing of PI-based LFC system. To tune the PI parameters, the optimal H_∞ control is used via a multiconstraint minimization problem. The problem formulation is based on expressing the constraints as an LMI, which can be easily solved using available semidefinite programming methods [8].

Unfortunately, in the presence of strong constraints and tight objective conditions, because of following reasons, the addressed optimization theorem in [7] may not reach a strictly feasible solution for a given time-delayed LFC system and a more comprehensive/flexible control design algorithm is needed.

- 1) Naturally, LFC is a multiobjective control problem. LFC goals, i.e., frequency regulation and tracking the load changes, maintaining the tie-line power interchanges to specified values in the presence of generation constraints and time delays, determines the LFC synthesis as a multiobjective control problem. Therefore, it is expected that an appropriate multiobjective control strategy (such as the mixed H_2/H_∞ control technique) could be able to give a better solution for this problem than a single-norm control method (for example, H_∞ control).
- 2) Although the proposed H_∞ PI-based LFC design in [7] gives a simple design procedure, as shown in the mentioned paper, the necessary condition for the existence of the solution is that the nominal system transfer function must be strictly positive real (SPR) [9]. This condition limits the application of addressed control strategy to a class of dynamical power systems.
- 3) It is significant to note that because of the use of simple constant gains, pertaining to optimal static output feedback (SOF) synthesis for dynamical systems in the presence of strong constraints and tight objectives are few and restrictive. Under such conditions, the given minimization problem in [7] may not reach an optimal solution for the all assumed dynamic LFC systems (such as the considered case study in the present paper).

Manuscript received November 29, 2006; revised July 11, 2007. First published January 13, 2009; current version published February 19, 2009. This work was supported in part by the Japan Society for the Promotion of Science (JSPS) under Grant P04346 and in part by the University of Kurdistan. Paper no. TEC-00565-2006.

H. Bevrani is with the Department of Electrical and Computer Engineering, University of Kurdistan, Sanandaj, 416, Kurdistan, Iran (e-mail: bevrani@uok.ac.ir).

T. Hiyama is with the Department of Electrical and Computer Engineering, Kumamoto University, Kumamoto 860-8555, Japan (e-mail: hiyama@eecs.kumamoto-u.ac.jp).

Color versions of one or more of the figures in this paper are available online at <http://ieeexplore.ieee.org>.

Digital Object Identifier 10.1109/TEC.2008.2003205

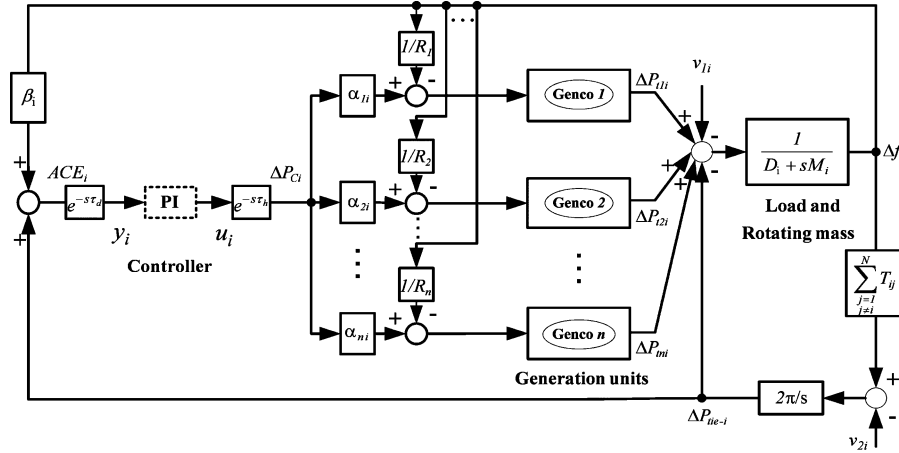


Fig. 1. General control area with time delays.

In this paper, a more relaxed control strategy is introduced to invoke the strict-positive realness condition, and to cover all of the LFC performance targets. The PI-based multidelayed LFC problem is transferred to an SOF control design. The time delay is considered as a model uncertainty, and the mixed H_2/H_∞ control is used via an iterative linear matrix inequalities (ILMIs) algorithm to approach a suboptimal solution for the specified LFC design objectives. Simplicity of control structure, keeping the fundamental LFC concepts, using multidelay-based LFC system, applicable for a wide range of LFC systems, and no need for an additional controller can be considered as advantages of the present LFC design methodology in comparison to existing methods. To demonstrate the efficiency of the proposed control method, some real-time nonlinear laboratory tests have been performed on the analog power system simulator at the Research Laboratory, Kyushu Electric Power Company.

II. PROPOSED CONTROL STRATEGY

A. LFC With Time Delays

For the purpose of this research, the communication delays are considered on the control input and control output of the LFC system. Namely, the delays on the measured frequency and power tie-line flow from remote terminal units (RTUs) to the control center, which can be considered on the area control error (ACE) signal and the produced rise/lower signal from the control center to individual generation units.

The time-delayed LFC system is shown in Fig. 1. The parameters and labels are defined in the next section. The communication delay is expressed by an exponential function $e^{-s\tau}$, where τ gives the communication delay time. Following a load disturbance within a control area, the frequency of the area experiences a transient change, and the feedback mechanism comes into play and generates the appropriate control signal to make the generation readjust to meet the load demand. The balance between the connected control areas is achieved by detecting the frequency and tie-line power deviation via communication line, to generate the ACE signal used by the PI controller. The control signal is submitted to the participated generation companies (Gencos) via another communications link, based on their participation factors.

In this paper, the PI based LFC design objectives for a given control area can be summarized to synthesize a robust PI controller, maintain the system frequency, and tie-line power flows close to reference values in the presence of communication delays and a wide range of load changes and disturbances, considering the existing physical constraints.

The PI-based LFC problem can be easily transferred to an SOF control problem by augmenting the measured output signal to include the ACE and its integral

$$u(t) = ky(t) \quad (1)$$

$$u(t) = k_P ACE + k_I \int ACE = [k_P \quad k_I] \begin{bmatrix} ACE \\ \int ACE \end{bmatrix}^T \quad (2)$$

where k_P and k_I are constant real numbers (PI parameters). The main merit of this transformation is in the possibility of using the well-known SOF control techniques to calculate the fixed gains, and once the SOF gain vector is obtained, the PI gains are ready in hand and no additional computation is needed.

Using the described transformation from PI to SOF control design, the time-delayed LFC problem is reduced to the synthesis of SOF control for the time-delay system given in (1) and k is a static gain to be determined. An optimal LMI-based H_∞ solution is addressed in [7]. Practically, it is shown that a set of case studies does not satisfy the given necessary SPR condition in [7].

This paper addresses a more flexible methodology based on mixed H_2/H_∞ control technique. The time delay is considered as an uncertainty, and the stability and performance objectives are formulated via H_∞ and H_2 norms. Finally, a suboptimal solution is obtained using a developed ILMI algorithm.

B. Multiobjective PI-based LFC Design

Here, the LFC synthesis problem with time delay is formulated as a mixed H_2/H_∞ SOF control problem to obtain an appropriate PI controller. Specifically, the H_∞ performance is used to meet the robustness of the closed-loop system against communication delays, modeled as uncertainties. The H_2 performance is used to satisfy the other LFC performance objectives, e.g., minimizing the effects of load disturbances on area

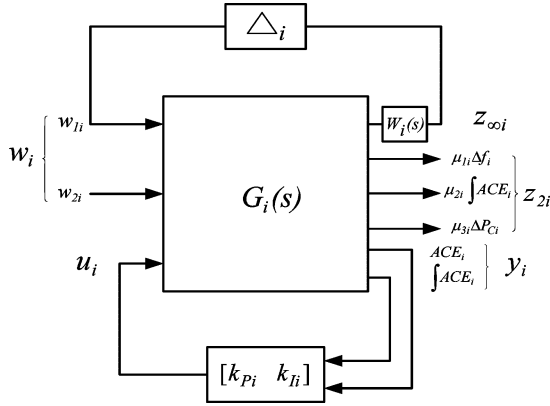


Fig. 2. H_2/H_∞ -SOF control framework.

frequency, ACE, and penalizing fast changes, and large overshoot on the governor load set point.

The overall control framework to formulate the time-delayed LFC problem via a mixed H_2/H_∞ control design is shown in Fig. 2. Using the standard simplified LFC model [10] for the prime mover and governor in Fig. 1, it is easy to find the state-space realization of each control area in the following form:

$$\begin{aligned} \dot{x}_i &= A_i x_i + B_{1i} w_i + B_{2i} u_i \\ z_{\infty i} &= C_{\infty i} x_i + D_{\infty 1i} w_i + D_{\infty 2i} u_i \\ z_{2i} &= C_{2i} x_i + D_{21i} w_i + D_{22i} u_i \\ y_i &= C_{yi} x_i + D_{y1i} w_i \end{aligned} \quad (3)$$

where x_i is the state variable vector, w_i is the disturbance or other external input vector, and y_i is the measured output vector. For a power system control area, the state variables can be considered as follows:

$$x_i^T = \left[\Delta f_i \quad \Delta P_{\text{tie}-i} \quad \int \text{ACE}_i \quad x_{ti} \quad x_{gi} \right] \quad (4)$$

where

$$\begin{aligned} x_{ti} &= [\Delta P_{t1i} \quad \Delta P_{t2i} \quad \cdots \quad \Delta P_{tni}] \\ x_{gi} &= [\Delta P_{g1i} \quad \Delta P_{g2i} \quad \cdots \quad \Delta P_{gni}] \end{aligned}$$

and

$$y_i^T = \left[\text{ACE}_i \quad \int \text{ACE}_i \right] \quad u_i = \Delta P_{Ci} \quad (5)$$

$$z_i^T = \left[\mu_{1i} \Delta f_i \quad \mu_{2i} \int \text{ACE}_i \quad \mu_{3i} \Delta P_{Ci} \right]. \quad (6)$$

Here, w_i can be obtained as follows:

$$w_i^T = [w_{1i} \quad w_{2i}] \quad w_{2i}^T = [v_{1i} \quad v_{2i}] \quad (7)$$

where w_{2i} is the fictitious perturbed input signal associated with the shown uncertainty loop in Fig. 2, and v_{1i} and v_{2i} demonstrate the area load disturbance and interconnection effects (area interface), respectively, and can be defined as follows:

$$v_{1i} = \Delta P_{di} \quad v_{2i} = \sum_{\substack{j=1 \\ j \neq i}}^N T_{ij} \Delta f_j \quad (8)$$

such that ΔP_{di} , T_{ij} , and Δf_i denote the area load disturbance, and tie-line synchronizing coefficient for areas i and j and frequency deviation, respectively. The ACE signal can be expressed as a linear combination of tie-line power change and frequency deviation

$$\text{ACE}_i = \beta_i \Delta f_i + \Delta P_{\text{tie}-i}. \quad (9)$$

The other variables and parameters (including those shown for the LFC system in Fig. 1) are defined as follows: ΔP_{gi} , governor valve position; ΔP_{Ci} , governor load set point; ΔP_{tki} , turbine power; $\Delta P_{\text{tie}-i}$, net tie-line power flow; M_i , equivalent inertia constant; D_i , equivalent damping coefficient; β_i , frequency bias; R_k , drooping characteristic; and α_{ki} , ACE participation factors.

The output channel $z_{\infty i}$ is associated with the H_∞ performance, while the fictitious output vector z_{2i} is associated with the linear quadratic Gaussian (LQG) aspects (H_2 performance). μ_{1i} , μ_{2i} , and μ_{3i} are constant weights that must be chosen by the designer to obtain the desired closed-loop performance. $G_i(s)$ is the nominal dynamic model of the given control area, y_i is the augmented measured output vector (performed by ACE and its integral), u_i is the control input, and w_i includes the perturbed and disturbance signals in the given control area.

Δ_i shows the uncertainty block corresponding to delayed terms and $W_i(s)$ is the associated weighting function. Here, time delays are considered as uncertainty. Unlike in [7], the delay elements do not directly appear in (3) and the LMIs in the coming pages.

The H_2 performance is used to minimize the effect of disturbances on area frequency and ACE by introducing appropriate fictitious controlled outputs. Furthermore, fictitious output $\mu_{3i} \Delta P_{Ci}$ sets a limit on the allowed control signal to penalize fast changes and large overshoot in the governor load set point, with regards to practical constraint on power generation by generator units [11]. The H_∞ performance is used to meet the robustness against specified uncertainties due to communication delays and reduction of its impact on the closed-loop system performance.

The PI-based LFC problem as a multiobjective SOF control design can be expressed to determine an admissible SOF law $K_i = [k_{Pi} \quad k_{Ii}]$, which belongs to a family of internally stabilizing SOF gains K_{sOF} ,

$$u_i = K_i y_i, \quad K_i \in K_{\text{sOF}} \quad (10)$$

such that

$$\inf_{K_i \in K_{\text{sOF}}} \|T_{z_{2i} w_{2i}}\|_2, \quad \text{subject to} \quad \|T_{z_{\infty i} w_{1i}}\|_\infty < 1 \quad (11)$$

where $T_{z_{\infty i} w_{1i}}$ and $T_{z_{2i} w_{2i}}$ are the transfer functions from w_{1i} and w_{2i} to $z_{\infty i}$ and z_{2i} , respectively.

C. Modeling of Uncertainties

For a given power system, the uncertainties due to time delays can be modeled as an unstructured multiplicative uncertainty block that contains all possible variation in the assumed delays range. Some methods to model the uncertainties in power systems are presented in [12] and [13]. Let $\hat{G}_i(s)$ denote the

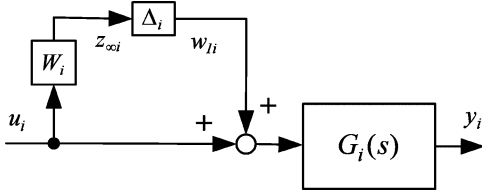


Fig. 3. Modeling the time delays as multiplicative uncertainty.

transfer function from the control input u_i to the control output y_i at operating points other than the nominal point. Then, we can represent this transfer function as

$$|\Delta_i(s)W_i(s)| = |[\hat{G}_i(s) - G_i(s)]G_i(s)^{-1}| \quad (12)$$

where

$$\|\Delta_i(s)\|_\infty = \sup_\omega |\Delta_i(s)| \leq 1; \quad G_i(s) \neq 0 \quad (13)$$

such that $\Delta_i(s)$ shows the uncertainty block corresponding to delayed terms and $G_i(s)$ is the nominal transfer function model. $W_i(s)$ is the associated weighting function such that its respective magnitude bode plot covers all possible time-delayed structures. Fig. 3 shows the simplified open-loop system after modeling the time delays as a multiplicative uncertainty.

D. Developed ILMI

The optimization problem given in (11) defines a robust performance synthesis problem where the H_2 -norm is chosen as the performance measure. Here, an ILMI algorithm is introduced to get a suboptimal solution for the aforementioned optimization problem. Specifically, the proposed algorithm formulates the H_2/H_∞ SOF control through a general SOF stabilization problem. The proposed algorithm searches the desired suboptimal H_2/H_∞ SOF controller K_i within a family of H_2 stabilizing controllers K_{sof} , such that

$$|\gamma_2^* - \gamma_2| < \varepsilon \quad \gamma_\infty = \|T_{z_{oi} w_{1i}}\|_\infty < 1 \quad (14)$$

where ε is a small real positive number, γ_2^* is H_2 performance corresponding to H_2/H_∞ SOF controller K_i , and γ_2 is the optimal H_2 performance index that can result from an application of standard H_2/H_∞ dynamic output feedback control.

In the proposed strategy, based on the generalized static output stabilization feedback lemma [14], first, the stability domain of (PI parameters) space, which guarantees the stability of the closed-loop system, is specified. In the second step, the subset of the stability domain in the PI parameter space is specified to minimize the H_2 tracking performance. Finally, as described in the authors' preliminary work [15], the design problem becomes determining the point with the closest H_2 performance index to the optimal one that meets the H_∞ constraint. The main effort is to formulate the H_2/H_∞ problem via the generalized static output stabilization feedback lemma, such that all eigenvalues of $(A-BKC)$ shift toward the left half-plane through the reduction of a_i , a real number, to close to feasibility of (11). The proposed algorithm includes the following steps.

Step 1) Compute the state-space model (3) for the given control system.

Step 2) Tune the constant weights and compute the optimal guaranteed H_2 performance index γ_2 using function *hinfmix* in MATLAB-based LMI control toolbox [16], to design a standard H_2/H_∞ dynamic output controller for the performed system in step 1.

Step 3) Set $i = 1$, $\Delta\gamma_2 = \Delta\gamma_0$, and let $\gamma_{2i} = \gamma_0 > \gamma_2$. $\Delta\gamma_0$ and γ_0 are positive real numbers. Select $Q = Q_0 > 0$, and solve X from the following algebraic Riccati equation:

$$A_i X + X A_i^T - X C_{yi}^T C_{yi} X + Q = 0, \quad X > 0. \quad (15)$$

Set $P_1 = X$.

Step 4) Solve the following optimization problem for X_i , K_i , and a_i : minimize a_i subject to the LMI constraints

$$\begin{bmatrix} A_i X_i + X_i A_i^T + B_{1i} B_{1i}^T + \sum_i B_{2i} K_i + X_i C_{yi}^T \\ (B_{2i} K_i + X_i C_{yi}^T)^T & -I \end{bmatrix} < 0 \quad (16)$$

$$\text{trace}(C_{2ic} X_i C_{2ic}^T) < \gamma_{2i} \quad (17)$$

$$X_i = X_i^T > 0 \quad (18)$$

where $\sum_i = -P_i C_{yi}^T C_{yi} X_i - X_i C_{yi}^T C_{yi} P_i + P_i C_{yi}^T C_{yi} P_i - a_i X_i$.

Denote a_i^* as the minimized value of a_i .

Step 5) If $a_i^* \leq 0$, go to step 9.

Step 6) For $i > 1$ if $a_{i-1}^* \leq 0$, $K_{i-1} \in K_{\text{sof}}$ and go to step 10. Otherwise go to step 7.

Step 7) Solve the following optimization problem for X_i and K_i : minimize $\text{trace}(X_i)$ subject to LMI constraints [(16)–(18)] with $a_i = a_i^*$. Denote X_i^* as the X_i that minimized $\text{trace}(X_i)$.

Step 8) Set $i = i + 1$ and $P_i = X_{i-1}^*$, then go to step 4.

Step 9) Set $\gamma_{2i} = \gamma_{2i} - \Delta\gamma_2$, $i = i + 1$. Then, do steps 3–5.

Step 10) If $\gamma_{\infty, i-1} = \|T_{z_{oi} w_{1i}}\|_\infty \leq 1$, K_{i-1} is a suboptimal H_2/H_∞ SOF controller and $\gamma_2^* = \gamma_{2i} - \Delta\gamma_2$ indicates a lower H_2 bound, such that the obtained controller satisfies (14). Otherwise go to 7.

III. REAL-TIME LABORATORY EXPERIMENT

A. Configuration of Study System

To illustrate the effectiveness of the proposed control strategy, a real-time experiment has been performed on the large scale analog power system simulator at the Research Laboratory, Kyushu Electric Power Company. For the purpose of this study, a longitudinal four-machine infinite bus system is considered as the test system. A single-line representation of the study system is shown in Fig. 4. All generator units are of thermal type, with separate conventional excitation control systems. The set of four generators represents a control area (area I), and the infinite bus is considered as other connected systems (area II).

The detailed block diagram of each generator unit and its associated turbine system (including the high-pressure, intermediate-pressure, and low-pressure parts) is illustrated in Fig. 5. The power system parameters are given in Table IV (see the Appendix).

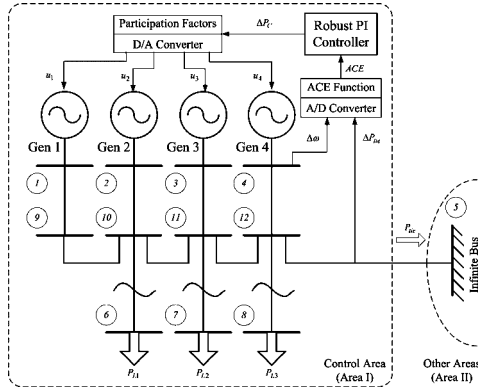


Fig. 4. Study power system.

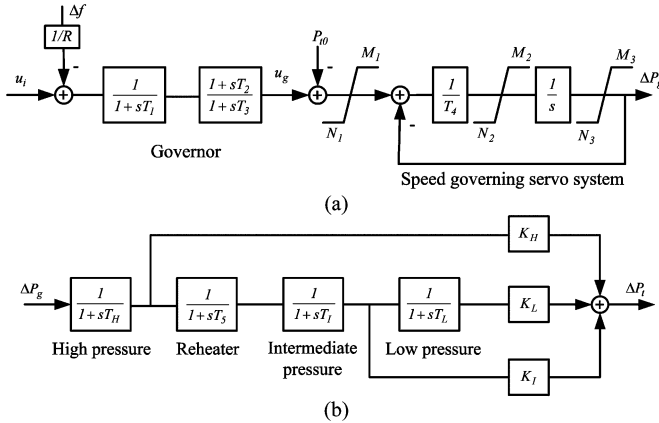


Fig. 5. Generator unit. (a) Speed governing system. (b) Detailed turbine system.

TABLE I
OSCILLATION MODES IN ACTUAL AND LABORATORY SYSTEMS

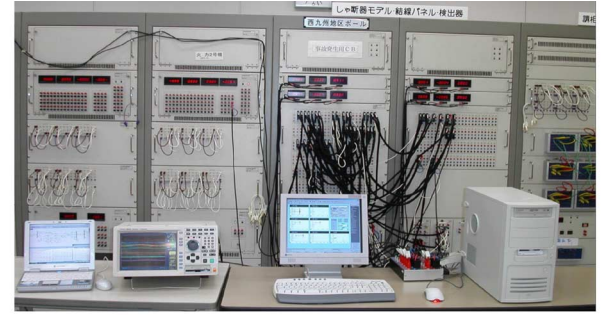
Power System	Global Osc. Mode	Local Osc. Mode
Actual WJPS	0.30 HZ	0.10-2.50 HZ
Laboratory System	0.30 HZ	0.15-2.40 HZ

Although, in the given model, the number of generators is reduced to 4, it closely represents the dynamic behavior of the West Japan Power System (WJPS). As shown in Table I, the most important global and local oscillation modes of the actual system are included. The essential global oscillation mode of the actual WJPS is around 0.3 Hz. Depending on the individual generators, the local oscillation modes are varied in the frequency range of 0.1–2.5 Hz. There also exists an interarea oscillation mode around 0.7 Hz.

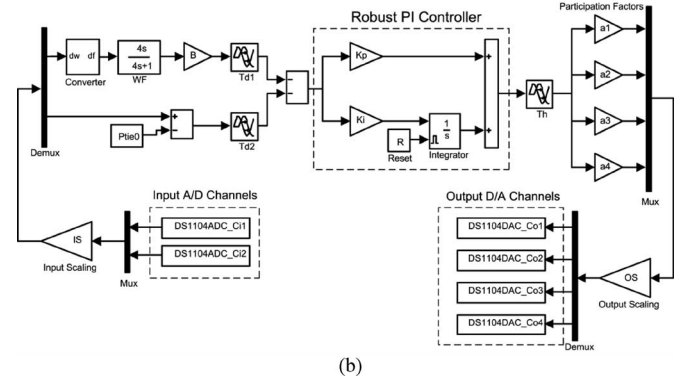
B. PI Controller

The proposed control loop including robust PI controller, ACE computing unit, and participation factors, which have been built in a personal computer [shown in the right side of Fig. 6(a)], were connected to the power system using a digital signal processing (DSP) board equipped with A/D and digital to analog (D/A) converters as the physical interfaces between the personal computer and the analog power system hardware.

Fig. 6(a) shows the overview of the applied laboratory experiment devices including the control/monitoring desks. The



(a)



(b)

Fig. 6. Performed laboratory experiment. (a) Control/monitoring desks. (b) PC-based implemented control loop.

PC-based control loop is shown in Fig. 6(b). A digital oscilloscope and a notebook computer [shown in the left side of Fig. 6(a)] are used for monitoring purposes.

Based on a simple stability condition [17], the open-loop system with real matrices is stable if

$$\mu(A) + \|A_d\| < 0 \quad (19)$$

where

$$\mu(A) = \frac{1}{2} \max_j \lambda_j(A^T + A). \quad (20)$$

Here, A_d is the associated delay term with the nominal system matrix A , and λ_j denote the j th eigenvalue of $(A^T + A)$. Using the previous stability rule, we note that for the present example, the control area is unstable ($\mu(A) + \|A_d\| = 11.0519 > 0$).

It is easy to show that the described H_∞ -based technique in [7] is not able to obtain a feasible optimal solution. In order to get a suboptimal solution, we apply the proposed control strategy given in Section II.

Some sample uncertainties due to delays variation, within the following range that is close to the real LFC cycle, are shown in Fig. 7.

$$\tau = \tau_d + \tau_h \in [0 \quad 8]s. \quad (21)$$

It should be noted that the shown uncertainty curves are drawn by solving (12) for different delay samples. The samples must be chosen among an admissible delay range. Finally, to keep the complexity of the design procedure simple, we model uncertainties from both delayed channels by using a low-order

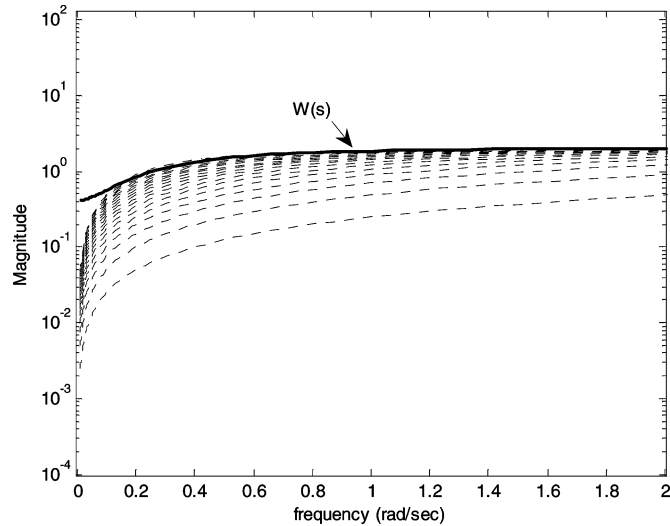


Fig. 7. Uncertainty plots (dotted) due to the communication delays and the upper bound (solid).

norm-bounded multiplicative uncertainty to cover all possible plants as follows:

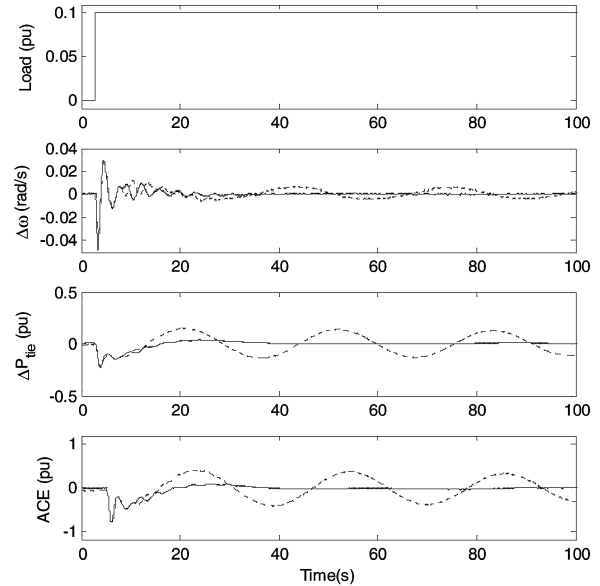
$$W(s) = \frac{2.1012s + 0.2130}{s + 0.5201}. \quad (22)$$

Fig. 7 clearly shows that the chosen first-order weight $W(s)$ provides a little conservative design at low frequencies; however, it provides a good tradeoff between robustness and design complexity. It is notable that using a high-order weighting function to find a tighter upper bound may result in a failure to obtain feasible optimal PI parameters. On the other hand, the determined low-order $W(s)$ must cover all the uncertainty curves. Otherwise, for the obtained PI parameters, the robustness cannot be guaranteed for all the specified delay changes.

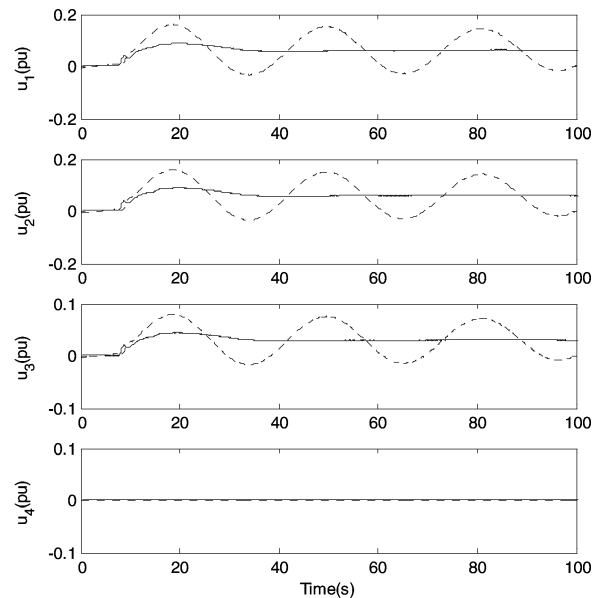
In the present example, the time delay of communication channels is considered near to the LFC cycle rate. A wider range of delays can be considered by choosing a larger τ . As a result, it provides a new upper bound for the modeled uncertainty without any change in the design procedure.

Considering the existing limits on the rate and range of generation change and the fact that the generation units (for example, steam units) need time to fully respond, the proposed control strategy includes enough flexibility to set a desired level of performance and cover practical constraint on the control action signal. This can be easily done by tuning the constant weights μ_i associated with the fictitious controlled outputs in Fig. 2.

For choosing the constant weights, one can fix the weights μ_{1i} , μ_{2i} , and μ_{3i} to unity and use the method with the regional pole placement technique for the purpose of performance tuning [18]. Here, since there are only three tunable parameters, the trial-and-error approach can be considered as an acceptable alternative method. The selection of these performance weights is dependent on specified LFC performance objectives. In fact, an important issue with regard to the selection of these weights is the degree to which they can guarantee the satisfaction of design performance objectives. The selection of weights entails a trade-off among several performance requirements. Coefficients μ_{1i}



(a)



(b)

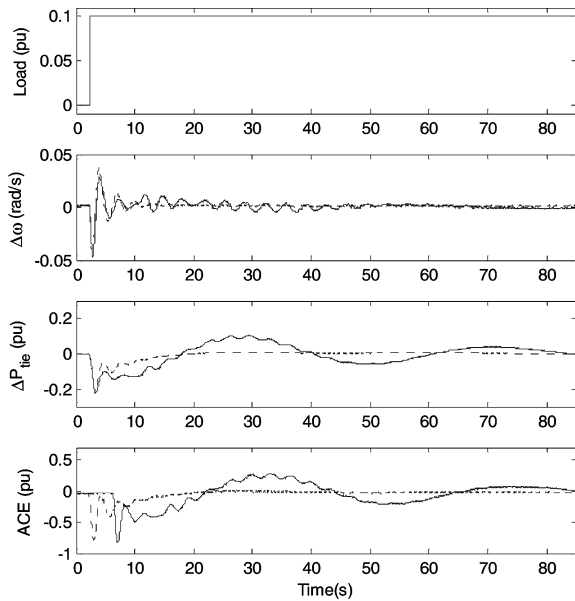
Fig. 8. System response for scenario 1 (5 s delay following a 0.1-p.u. step load increase), using proposed method (solid) and the design technique given in [19].

TABLE II
PARTICIPATION FACTORS IN SCENARIOS 1 AND 2

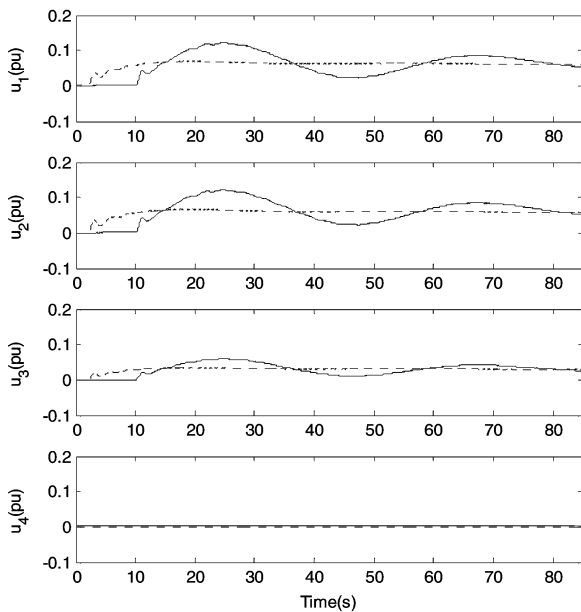
Gen. unit	1	2	3	4
α	0.4	0.4	0.2	0.0

and μ_{2i} at controlled outputs set the performance goals (tracking the load variation and disturbance attenuation), while μ_{3i} sets a limit on the allowed control action to penalize fast change and large overshoot in the governor load set-point signal.

Based on the earlier explanation and using the trial-and-error method for the present LFC system, values 0.5, 1, and 5 are chosen for the weights μ_{1i} , μ_{2i} , and μ_{3i} , respectively. Finally, according to the synthesis methodology described in Section II,



(a)



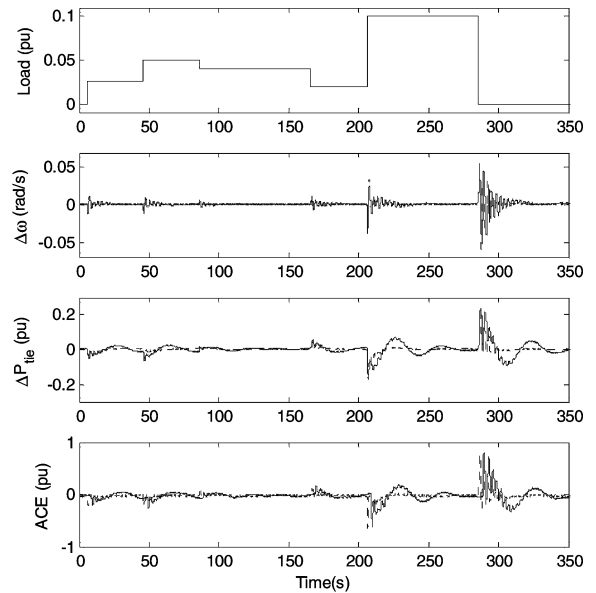
(b)

Fig. 9. System response for scenario 2: with 8-s delay (solid) and without delay (dotted), following a 0.1-p.u. step load increase.

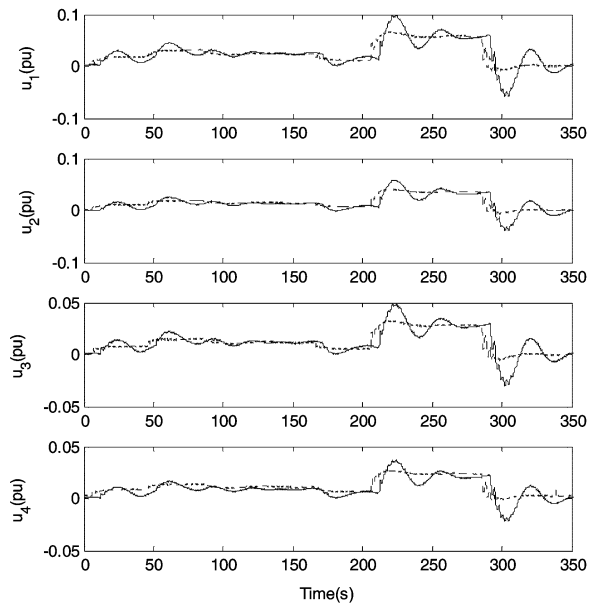
the parameters of the PI controller are obtained as $k_{P_i} = 0.3509$ and $k_{I_i} = 0.2104$.

IV. LABORATORY RESULTS

In the performed nonlinear real-time laboratory experiment, the proposed PI controller was applied to the control area power system described in Fig. 4. The performance of the closed-loop system is tested in the presence of load disturbances and time delays. The nominal area load demands that P_{L1} , P_{L2} , and P_{L3} (Fig. 4) during test scenarios are considered as 0.3, 0.6, and 0.6 per unit (p.u.), respectively.



(a)



(b)

Fig. 10. System response for scenario 3: with 6-s delay (solid) and without delay (dotted), following a sequence of step load changes.

For scenario 1, the power system is examined with delays, following a 0.1-p.u. step load increase in the control area. The total communication delay is assumed as 5 s. The closed-loop system response, including frequency deviation ($\Delta\omega$), tie-line power change (ΔP_{tie}), ACE, and control action signals (u_i) are shown in Fig. 8.

The system performance is compared with a designed robust H_∞ -PI controller based on the given methodology in [19] for the delay-less LFC systems. As shown in Fig. 8, using delay-less H_∞ design, the system falls in a critical condition and leads to an unstable operating point, while the proposed H_2/H_∞ -PI controller acts to return the frequency, tie-line power, and

TABLE III
PARTICIPATION FACTORS IN SCENARIO 3

Gen. unit	1	2	3	4
α	0.40	0.25	0.20	0.15

ACE signals to the scheduled values properly. Fig. 8 shows the changes in control signals applied to the generator units provided according to their participation factors listed in Table II.

In scenario 2, the power system was tested for a longer time delay. Fig. 9 shows the closed-loop response in the presence of 8-s total communication delay, following a 0.1-p.u. step load increase in the control area. In scenario 3, the system response was tested for a sequence of step load changes as shown in Fig. 10. The total delay was fixed at 6 s. The figures show that the frequency deviation and ACE of the control area are properly maintained within a narrow band using smooth control efforts. The participation factors for the recent experiment are given in Table III.

The obtained results show that the designed controllers can ensure good performance despite load disturbance and indeterminate delays in the communication network. It is shown that the robust PI controller acts to maintain area frequency and total exchange power close to the scheduled values by sending a corrective smooth signal to the gencos in proportion to their participation in the LFC task.

Considering the time delays as structured uncertainties, the mentioned method provides a conservative design, but it gives a good tradeoff among the specified LFC objectives using the H_2 and H_∞ performances. The experiment results show that this controller performs well for a wide range of operating conditions, considering the load fluctuation and communication delays.

V. CONCLUSION

The PI-based LFC problem with communication delays in a multiarea power system is formulated as a robust SOF optimization control problem. To obtain the constant gains, a flexible methodology is developed to invoke the existing strictness. The time delay is considered as a model uncertainty and the H_2/H_∞ control is used via an ILMIs algorithm to approach a suboptimal solution for the assumed design objectives. The proposed method was applied to a control area power system through a laboratory real-time experiment.

In the proposed LFC methods, an important goal was to keep the simplicity of control algorithms (as well as control structure) for computing the PI parameters among the well-known LFC scheme. For the reasons of simplicity, flexibility, and straightforwardness of the control algorithms, we hope this paper acts as a catalyst to bridge the robust control theory—real world LFC gap as well as the classical—modern LFC design gap.

APPENDIX

The power system parameters for the performed laboratory tests are given in Table IV.

TABLE IV
POWER SYSTEM PARAMETERS

Parameter	Gen 1	Gen 2	Gen 3	Gen 4
MVA	1000	600	1000	900
R (Hz/pu)	3.00	3.00	3.30	3.30
T_1 (Sec)	0.08	0.06	0.07	0.07
T_2 (Sec)	0.10	0.10	0.10	0.10
T_3 (Sec)	0.10	0.10	0.10	0.10
T_4 (Sec)	0.40	0.36	0.42	0.3
T_5 (Sec)	10.0	10.0	10.0	10.0
β (pu/Hz)	0.3483	0.3473	0.3180	0.3827
D (pu/Hz)	0.0150	0.0150	0.0150	0.0150
M (Sec)	8.05	7.00	8.05	6.00
T_H (Sec)	0.05	0.05	0.05	0.05
T_I (Sec)	0.08	0.08	0.08	0.08
T_L (Sec)	0.58	0.58	0.58	0.58
K_H (pu)	0.31	0.31	0.31	0.31
K_I (pu)	0.24	0.24	0.24	0.24
K_L (pu)	0.45	0.45	0.45	0.45
M_1 (pu/Minute)	0.50	0.50	0.50	0.50
M_2 (pu/Minute)	0.050	0.050	0.050	0.050
M_3 (pu/Minute)	2.00	2.00	2.00	2.00
N_1 (pu/Minute)	-0.50	-0.50	-0.50	-0.50
N_2 (pu/Minute)	-0.20	-0.20	-0.20	-0.20
N_3 (pu/Minute)	-0.50	-0.50	-0.50	-0.50

ACKNOWLEDGMENT

The authors would like to thank N. Wakasugi, A. Matsunaga, Y. Fujimoto, T. Kouichi, Y. Hirofumi, and K. Hiroyuki for their help in making a successful experiment in the Research Laboratory, Kyushu Electric Power Company.

REFERENCES

- [1] M. S. Mahmoud, *Robust Control and Filtering for Time-Delay Systems*. New York: Marcel Dekker, 2000.
- [2] J. Aweya, D. Y. Montuno, and M. Ouellette, "Effects of control loop delay on the stability of a rate control algorithm," *Int. J. Commun. Syst.*, vol. 17, pp. 833–850, 2004.
- [3] S. I. Niculescu, *Delay Effects on Stability—A Robust Control Approach*. New York: Springer-Verlag, 2001.
- [4] S. Bhowmik, K. Tomosovic, and A. Bose, "Communication models for third party load frequency control," *IEEE Trans. Power Syst.*, vol. 19, no. 1, pp. 543–548, Feb. 2004.
- [5] T. Hiyama, T. Nagata, and T. Funabashi, "Multi-agent based automatic generation control of isolated stand alone power system," in *Proc. Int. Conf. Power Syst. Technol.*, vol. 1, 2004, pp. 139–143.
- [6] X. Yu and K. Tomosovic, "Application of linear matrix inequalities for load frequency control with communication delays," *IEEE Trans. Power Syst.*, vol. 19, no. 3, pp. 1508–1515, Aug. 2004.
- [7] H. Bevrani and T. Hiyama, "Robust load-frequency regulation: A real-time laboratory experiment," *Optimal Control Appl. Methods*, vol. 28, no. 6, pp. 419–433, 2007.
- [8] S. Boyd, L. El. Ghaoui, E. Feron, and V. Balakrishnan, *Linear Matrix Inequalities in Systems and Control Theory*. vol. 15, Philadelphia, PA: SIAM Books, 1994.
- [9] K. S. Narendra and A. M. Annaswamy, *Stable Adaptive Systems*. Englewood Cliffs, NJ: Prentice-Hall, 1989.
- [10] A. J. Wood and B. F. Wollenberg, *Power Generation Operation and Control*. New York: Wiley, 1984.

- [11] N. Jaleeli, D. N. Ewart, and L. H. Fink, "Understanding automatic generation control," *IEEE Trans. Power Syst.*, vol. 7, no. 3, pp. 1106–1112, Aug. 1992.
- [12] M. Djukanovic, M. Khammash, and V. Vittal, "Sequential synthesis of structured singular value based decentralized controllers in power systems," *IEEE Trans. Power Syst.*, vol. 4, no. 2, pp. 635–641, May 1999.
- [13] M. Rios, N. Hadjsaid, R. Feuillet, and A. Torres, "Power system stability robustness evaluation by analysis," *IEEE Trans. Power Syst.*, vol. 14, no. 2, pp. 648–653, May 1999.
- [14] Y. Y. Cao, J. Lam, Y. X. Sun, and W. J. Mao, "Static output feedback stabilization: An ILMI approach," *Automatica*, vol. 34, no. 12, pp. 1641–1645, 1998.
- [15] H. Bevrani and T. Hiyama, "A control strategy for LFC design with communication delays," in *Proc. Power Eng. Conf.*, Singapore, 2005, pp. 1–6.
- [16] P. Gahinet, A. Nemirovski, A. J. Laub, and M. Chilali, *LMI Control Toolbox*. Natick, MA: The MathWorks, 1995.
- [17] T. Mori and H. Kokame, "Stability of $\dot{x}(t) = Ax(t) + Bx(t - \tau)$," *IEEE Trans. Autom. Control*, vol. 34, no. 4, pp. 460–462, Apr. 1989.
- [18] P. Gahinet and M. Chilali, " H_∞ -design with pole placement constraints," *IEEE Trans. Autom. Control*, vol. 41, no. 3, pp. 358–367, Mar. 1996.
- [19] H. Bevrani, Y. Mitani, and K. Tsuji, "Robust decentralized load-frequency control using an iterative linear matrix inequalities algorithm," *Inst. Electr. Eng. Proc. Gener. Transm. Distrib.*, vol. 150, no. 3, pp. 347–354, 2004.



Hassan Bevrani (S'90–M'04–SM'08) was born in Kurdistan, Iran. He received the M.Eng. (Hons.) degree from K. N. Toosi University of Technology, Tehran, Iran, in 1997, and the Ph.D. degree from Osaka University, Osaka, Japan, in 2004, both in electrical engineering.

From 2004 to 2006, he was a Postdoctoral Fellow at Kumamoto University, Kumamoto, Japan. From 2007 to 2008, he was a Senior Research Fellow at Queensland University of Technology, Brisbane, Qld., Australia. He is currently an Assistant Professor at the University of Kurdistan, Sanandaj, Iran. His current research interests include robust load–frequency control and robust/intelligent control applications in power system and power electronic industry.

Prof. Bevrani is a member of the Institute of Electrical Engineers of Japan and the Institution of Engineering and Technology (IET).



Takashi Hiyama (M'86–SM'93) was born in Japan. He received the B.E., M.S., and Ph.D. degrees in electrical engineering from Kyoto University, Kyoto, Japan, in 1969, 1971, and 1980, respectively.

Since 1989, he has been a Professor in the Department of the Electrical and Computer Engineering, Kumamoto University, Kumamoto, Japan. His current research interests include the application of intelligent systems to power system operation, management, and control.

Prof. Hiyama is a member of the Institute of Electrical Engineers of Japan, the Society of Instrument and Control Engineers (SICE) of Japan, and the Japan Solar Energy Society.